PLUTO'S ATMOSPHERE FROM STELLAR OCCULTATIONS IN 2012 AND 2013

Alex Dias de Oliveira

Sicardy, B., Lellouch, E., Vieira-Martins, R., Assafin, M., Camargo, J. I. B.,J. I. B., Braga-Ribas, F., Gomes-Júnior, A. R., Benedetti-Rossi, G., Colas, F., Decock, A., Doressoundiram, A., Dumas, C., Emilio, M., Fabrega Polleri, J., Gil-Hutton, R., Gillon, M., Girard, J., Hau, G. K. T., Ivanov, V. D., Jehin, E., Lecacheux, J., Leiva, R. Lopez-Sisterna, C., Mancini, L., Manfroid, J., Maury, A., Meza, E., Morales, N., Nagy, L., Opitom, C., Ortiz, J. L., Pollock, J., Roques, F., Snodgrass, C., Soulier, J.F., Thirouin, A., Vanzi, L., Widemann, T., Reichart, D. E., LaCluyze, A. P., Haislip, J. B., Ivarsen, K. M., Dominik, M., Jørgensen, U., Skottfelt, J.

Summary

- Introduction
- Events (Prediction, Observation and Calibration)
- Modeling
- General atmospheric structure
- Stratosphere
- Mesosphere negative temperature gradient
- Conclusions

Why study Pluto's atmosphere?

- **Low incidence of solar radiation** - Origin and evolution of the Solar System.

Why study Pluto's atmosphere?

- **Low incidence of solar radiation** - Origin and evolution of the Solar System.
- **Atmospheric structure** - Correct interpretation of observational data (spectra).

Why study Pluto's atmosphere?

- **Low incidence of solar radiation** - Origin and evolution of the Solar System.
- **Atmospheric structure** - Correct interpretation of observational data (spectra).
- **Appearance and maintenance of atmospheres** - Other trans-neptunian objects with size and surface gravity comparable to those of Pluto within a factor of two, exihibited none atmosphere at the 10 nbar pressure level.

How to study it?

- **Direct Observation** - Spectroscopy. Information about the atmosphere and surface chemichal composition, and surface temperature.

How to study it?

- **Direct Observation** - Spectroscopy. Information about the atmosphere and surface chemichal composition, and surface temperature.
- **Indirect Observation** - Stellar occultations. High precision density, pressure and temperature profiles. Gravity waves (turbulence). Surface radius and composition (Combined with spectroscopy information).

Stellar Occultaions

- Consists into analyze the time variation of the star light, while crossing the atmosphere of the occulting object.

Stellar Occultaions

- Consists into analyze the time variation of the star light, while crossing the atmosphere of the occulting object.
- As far as ground based observations are concern, it is the most effective technique available to study Pluto's atmosphere. It allows an atmospheric probe to nbar levels (Sicardy et al., 2011; Olkin et al., 2014).

Stellar Occultations

- Responsable for Pluto's atmosphere discovery (Hubbard et al., 1988; Elliot et al., 1989; Brosch, 1995).

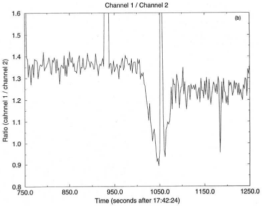

Brosch 95

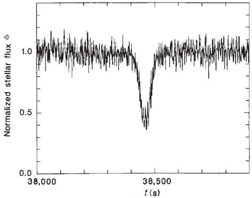

Hubbard 88

Elliot 89

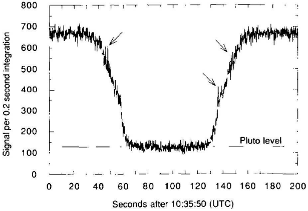

Prediction

- **Prediction catalog** - Assafin et al. (2010) Observed Pluto's path in the sky plane bewteen 2008 e 2015, performed at ESO's 2,2 m telescope.

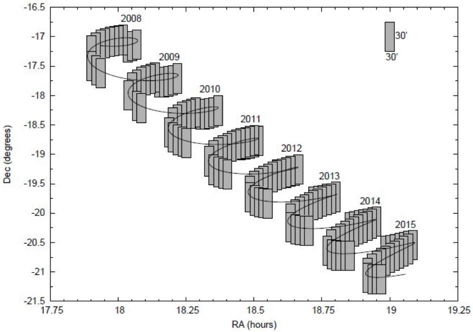

Prediction

- Predicted events observed at South America with ESO's 8.2 m VLT, among others.

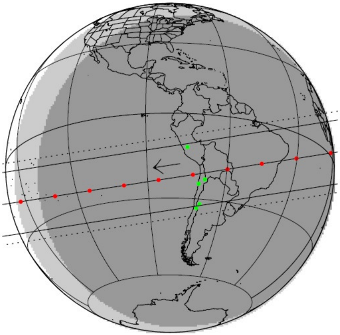

July 18, 2012 - R* 14

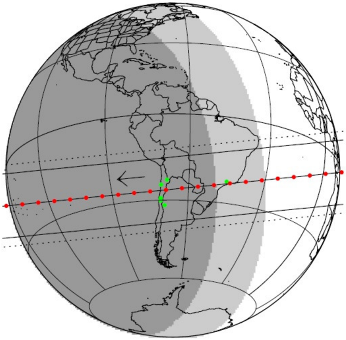

May 4, 2013 - R* 13,7

Observation

- **Event** - July 18, 2012.

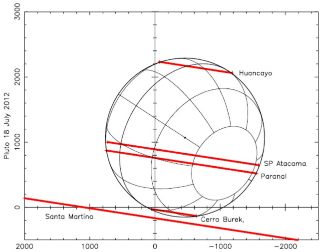

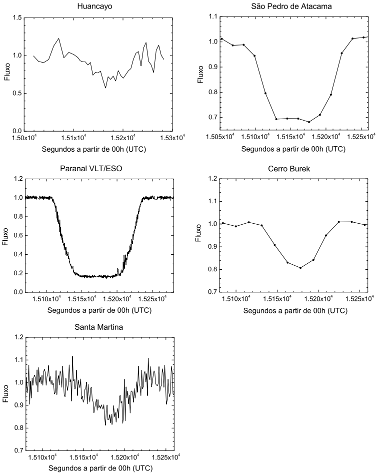

Observation

- **Event** - May 4, 2013.

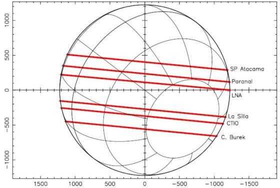

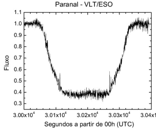

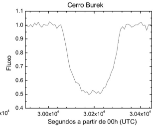

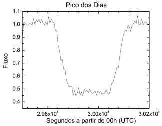

São Pedro de Atacama

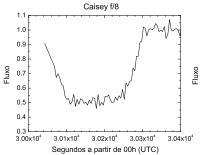

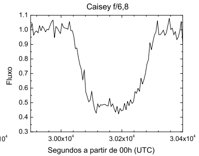

La Silla

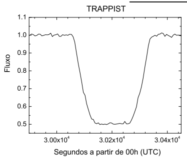

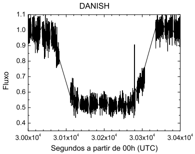

Cerro Tololo

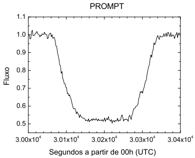

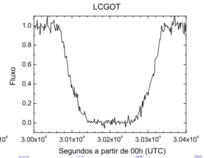

Calibration

- Digital coronography for calibration.

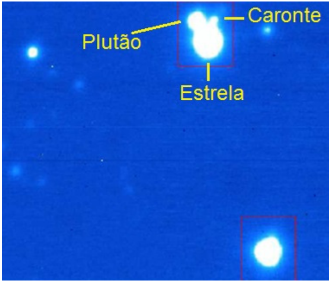

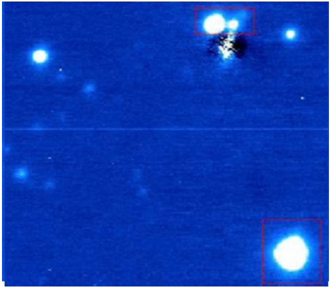

Calibration

- Stellar residual flux varied from 2.3 % to 1.8 % of its unocculted value.

18 July 2012 NACO

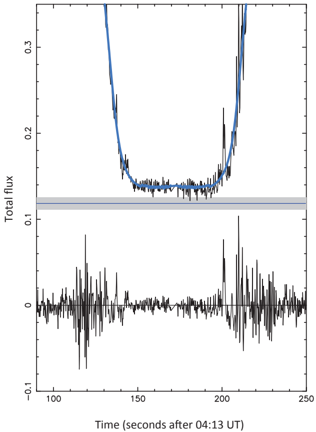

General Idea

- Assuming a layer model, a incident light ray suffers successives refractions, curving in the atmosphere until emerge.

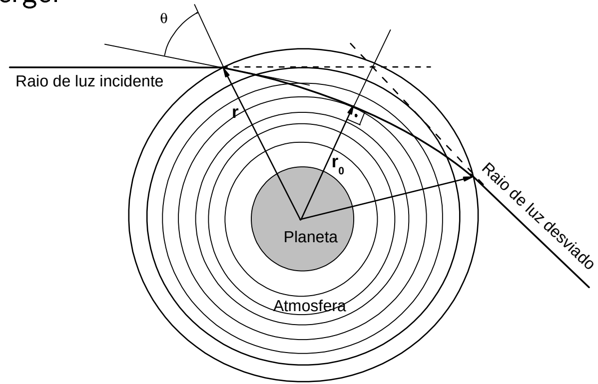

General Idea

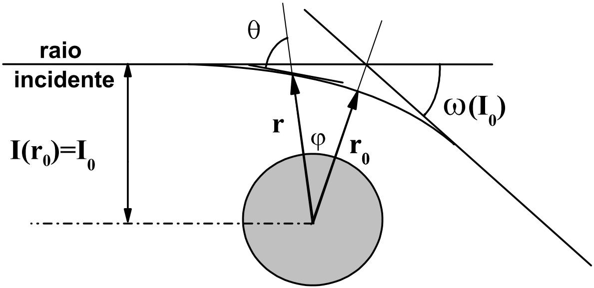

$$I(r_0) = \eta(r) \cdot r \cdot sen\theta$$

General Model

- Total deviation $\omega(r_0)$ is (Vapillon et al., 1973):

$$\omega(l_0) = \int_{r_0}^{\infty} \frac{2l_0}{\eta(r)} \cdot \frac{d\eta(r)}{dr} \cdot \frac{dr}{\sqrt{[\eta(r) \cdot r]^2 - [\eta(r_0) \cdot r_0]^2}} \qquad (1)$$

General Model

- Total deviation $\omega(r_0)$ is (Vapillon et al., 1973):

$$\omega(l_0) = \int_{r_0}^{\infty} \frac{2l_0}{\eta(r)} \cdot \frac{d\eta(r)}{dr} \cdot \frac{dr}{\sqrt{[\eta(r)\cdot r]^2 - [\eta(r_0)\cdot r_0]^2}} \qquad (1)$$

- Inverting for $\eta(r_0)$:

$$\eta(r_0) = exp\left\{\frac{1}{\pi}\int_{\omega(l_0)}^{0} \log\left[\frac{I(\omega)}{l_0} + \sqrt{\left(\frac{I(\omega)}{l_0}\right)^2 - 1}\right]\cdot d\omega\right\} \quad (2)$$

General Model

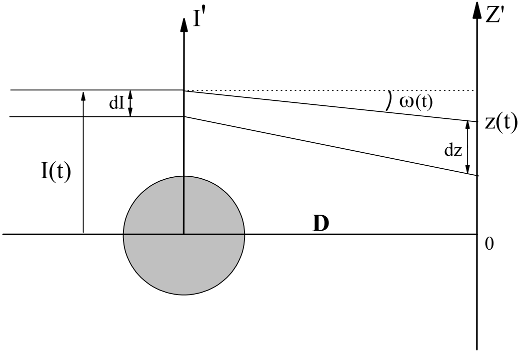

For small $\omega(r_0)$:

$$z(t) = I(t) + D \cdot \omega(t) \tag{3}$$

General Model

- By energy conservation we can write:

$$\frac{\Phi(t)}{\Phi_0} = \frac{dI(t)}{dz(t)} \quad (4)$$

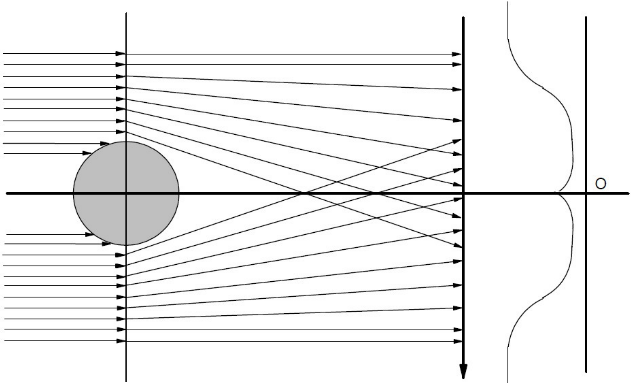

General Model

$$\frac{\Phi(t)}{\Phi_0} = f \cdot \frac{dI(t)}{dz(t)} \text{ where } f = I(t)/z(t) \tag{5}$$

$$\omega(t) = \frac{1}{D} \cdot \int_{-\infty}^{t} \frac{f \cdot \Phi_0 - \Phi(\tau)}{f \cdot \Phi_0} \cdot \frac{dz}{d\tau} d\tau \tag{6}$$

Reduction Approaches

Inversion:

- From the event data ($\Phi(t)/\Phi_0$ and $z(t)$), we calculate $I(t)$ e $\omega(t)$.

Reduction Approaches

Inversion:

- From the event data ($\Phi(t)/\Phi_0$ and $z(t)$), we calculate $I(t)$ e $\omega(t)$.
- From general model (Vapillon et al., 1973), we use $I(t)$ and $\omega(t)$ to get $\eta(r)$.

Reduction Approaches

Inversion:

- From the event data ($\Phi(t)/\Phi_0$ and $z(t)$), we calculate $I(t)$ e $\omega(t)$.
- From general model (Vapillon et al., 1973), we use $I(t)$ and $\omega(t)$ to get $\eta(r)$.
- From $\eta(r)$, we use a atmospheric model (assumptions) to determine $T(r)$, $n(r)$ e $P(r)$.

General Idea

Ray Tracing:

- From an atmospheric model ($T(r)$, $n(r)$ e $P(r)$) we calculate $\eta(r)$.

General Idea

Ray Tracing:

- From an atmospheric model ($T(r)$, $n(r)$ e $P(r)$) we calculate $\eta(r)$.
- Using $\eta(r)$ and the general model, we have $\omega(I_0)$ for each $I(t)$.

General Idea

Ray Tracing:

- From an atmospheric model ($T(r)$, $n(r)$ e $P(r)$) we calculate $\eta(r)$.
- Using $\eta(r)$ and the general model, we have $\omega(l_0)$ for each $l(t)$.
- From values of $l(t)$ and $\omega(t)$ We calculate synthetic values for $\Phi(t)/\Phi_0$ and $z(t)$.

Simplifying assumptions

- Pluto and its atmosphere are spherically symmetric.

Simplifying assumptions

- Pluto and its atmosphere are spherically symmetric.
- The atmosphere is Transparent (no Haze).

Simplifying assumptions

- Pluto and its atmosphere are spherically symmetric.
- The atmosphere is Transparent (no Haze).
- The atmosphere is an ideal gas in hydrostatic equilibrium.

Simplifying assumptions

- Pluto and its atmosphere are spherically symmetric.
- The atmosphere is Transparent (no Haze).
- The atmosphere is an ideal gas in hydrostatic equilibrium.

$$P(r) = k \cdot T(r) \cdot n(r) \quad \text{and} \quad \frac{dP}{dr} = -\mu \cdot n(r) \cdot g(r) \quad (7)$$

Simplifying assumptions

- Pluto and its atmosphere are spherically symmetric.
- The atmosphere is Transparent (no Haze).
- The atmosphere is an ideal gas in hydrostatic equilibrium.

$$P(r) = k \cdot T(r) \cdot n(r) \quad \text{and} \quad \frac{dP}{dr} = -\mu \cdot n(r) \cdot g(r) \quad (7)$$

$$\frac{1}{n} \cdot \frac{dn}{dr} = -\left[\frac{\mu \cdot g(r)}{k \cdot T} + \frac{1}{T} \cdot \frac{dT}{dr}\right] \qquad (8)$$

where

$$g(r) = \frac{GM}{r^2}$$

Simplifying assumptions

- Pluto and its atmosphere are spherically symmetric.
- The atmosphere is Transparent (no Haze).
- The atmosphere is an ideal gas in hydrostatic equilibrium.

$$P(r) = k \cdot T(r) \cdot n(r) \quad \text{and} \quad \frac{dP}{dr} = -\mu \cdot n(r) \cdot g(r) \quad (7)$$

$$\frac{1}{n} \cdot \frac{dn}{dr} = -\left[\frac{\mu \cdot g(r)}{k \cdot T} + \frac{1}{T} \cdot \frac{dT}{dr}\right] \quad (8)$$

where

$$g(r) = \frac{GM}{r^2}$$

Simplifying assumptions

- Is a pure molecular nitrogen (N_2) atmosphere. Other minor species, like methane, are neglected. Defining refractivity as:

Simplifying assumptions

- Is a pure molecular nitrogen (N_2) atmosphere. Other minor species, like methane, are neglected. Defining refractivity as:

$$\nu(r) = \eta(r) - 1;$$

Simplifying assumptions

- Is a pure molecular nitrogen (N_2) atmosphere. Other minor species, like methane, are neglected. Defining refractivity as:

$$\nu(r) = \eta(r) - 1;$$

$$\nu(r) = K \cdot n(r)$$

Simplifying assumptions

- Is a pure molecular nitrogen (N_2) atmosphere. Other minor species, like methane, are neglected. Defining refractivity as:

$$\nu(r) = \eta(r) - 1;$$

$$\nu(r) = K \cdot n(r)$$

$$K_N = 1{,}091 \cdot 10^{-23} + \frac{6{,}282 \cdot 10^{-26}}{\lambda^2} (cm^3/\text{molécula})$$

Simplifying assumptions

- Is a pure molecular nitrogen (N_2) atmosphere. Other minor species, like methane, are neglected. Defining refractivity as:

$$\nu(r) = \eta(r) - 1;$$

$$\nu(r) = K \cdot n(r)$$

$$K_N = 1{,}091 \cdot 10^{-23} + \frac{6{,}282 \cdot 10^{-26}}{\lambda^2} (cm^3/\text{molécula})$$

- $T(r)$ is time-independedt, i.e. the temperature profiles are the same in 2012 and 2013.

Iterative Procedure.

Iterative Procedure.

- Invert our best signal-to-noise ratio light curve to retrieve density, pressure and temperature profiles ($n(r)$, $P(r)$, and $T(r)$).

Iterative Procedure.

- Invert our best signal-to-noise ratio light curve to retrieve density, pressure and temperature profiles ($n(r)$, $P(r)$, and $T(r)$).
- With a parametrized $T(r)$ we generate, through direct ray tracing, synthetic occultation light-curves.

Iterative Procedure.

- Invert our best signal-to-noise ratio light curve to retrieve density, pressure and temperature profiles ($n(r)$, $P(r)$, and $T(r)$).
- With a parametrized $T(r)$ we generate, through direct ray tracing, synthetic occultation light-curves.
- They are simultaneously fitted to all the observed light-curves to pin down the location of Pluto's shadow center relative to the occultation chords for both events and the vertical position of temperature profile.

Iterative Procedure.

- Invert our best signal-to-noise ratio light curve to retrieve density, pressure and temperature profiles ($n(r)$, $P(r)$, and $T(r)$).
- With a parametrized $T(r)$ we generate, through direct ray tracing, synthetic occultation light-curves.
- They are simultaneously fitted to all the observed light-curves to pin down the location of Pluto's shadow center relative to the occultation chords for both events and the vertical position of temperature profile.
- With new shadow's center coordinates, the inversion of the best light-curve is performed again and the procedures ir resumed.

Combining the data

- Inversion of the light curve from VLT/ESO July 18, 2012 event, give a temperature profile $T(r)$.

Combining the data

- Inversion of the light curve from VLT/ESO July 18, 2012 event, give a temperature profile $T(r)$.
- From a parametric form of $T(r)$, we do a ray tracing for May 4, 2013 event, from which we get the inicial position $(r_i = r_1)$ of the temperature profile.

Combining the data

- Inversion of the light curve from VLT/ESO July 18, 2012 event, give a temperature profile $T(r)$.
- From a parametric form of $T(r)$, we do a ray tracing for May 4, 2013 event, from which we get the inicial position $(r_i = r_1)$ of the temperature profile.
- Using the calculated r_i we redo the ray tracing for the July 18, 2012 event to determine P_i and the shadows center coordinates.

Combining the data

- Inversion of the light curve from VLT/ESO July 18, 2012 event, give a temperature profile $T(r)$.
- From a parametric form of $T(r)$, we do a ray tracing for May 4, 2013 event, from which we get the inicial position $(r_i = r_1)$ of the temperature profile.
- Using the calculated r_i we redo the ray tracing for the July 18, 2012 event to determine P_i and the shadows center coordinates.
- We new center coordinates $(z(t))$ we redo July 18, 2012 event inversion to ger a precise temperature profile.

Parametrization of $T(r)$

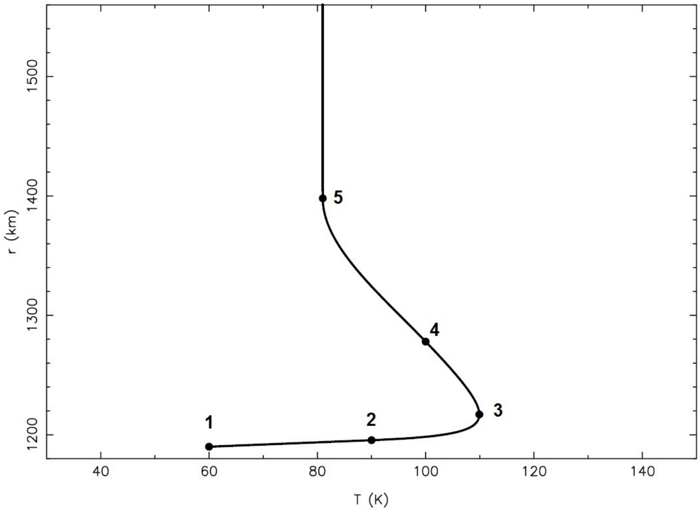

Parametrization of $T(r)$

$$
\begin{cases}
T(r) = T_1 + \frac{dT}{dr} \cdot (r - r_1), & r \leq r_2 \\
C_1 \cdot r + C_2 \cdot T(r) + C_3 \cdot r \cdot T(r) + C_4 \cdot r^2 + C_5 \cdot T(r)^2 = 1, & r_2 \leq r \leq r_4 \\
T(r) = C_6 + C_7 \cdot r + C_8 \cdot r^2 + C_9 \cdot r^3, & r_4 \leq r \leq r_5 \\
T(r) = T_{iso} & r \geq r_5
\end{cases}
\tag{9}
$$

Final Temperature Profile

Physical parameters		
Pluto's mass[1]	$GM = 8.703 \times 10^{11}$ m^3 s^{-2}	
Nitrogen molecular mass[2]	$\mu = 4.652 \times 10^{-26}$ kg	
Nitrogen molecular refractivity[3]	$K = 1.091 \times 10^{-23} + (6.282 \times 10^{-26}/\lambda^2_{\mu m})$ cm^3 molecule^{-1}	
Boltzmann constant	$k = 1.380626 \times 10^{-23}$ J K^{-1}	
The nine free parameters of the best temperature profile[4]		
r_1, T_1, $dT/dr(r_1)$	$1,190.4 \pm 1$ km, 36 K, 16.9 K km^{-1}	
r_2, T_2	$1,217.3$ km, 109.7 K	
r_3, T_3	$1,302.4$ km, 95.5 K (implying $dT/dr(r_3) = -0.206$ K km^{-1})	
r_4, T_4	$1,392.0$ km, 80.6 K	
$c1, c2$	$1.41397736 \times 10^{-3}$, $2.59861886 \times 10^{-3}$	
$c3, c4$	$-2.19756021 \times 10^{-6}$, $-4.81764971 \times 10^{-7}$	
$c5, c6$	$8.66619700 \times 10^{-8}$, -3.6213609×10^{4}	
$c7, c8$	8.2775269×10^{1}, $-6.27372563 \times 10^{-2}$	
$c9$	$1.58068760 \times 10^{-5}$	
The three free parameters particular to each event[5]		
	18 July 2012	04 May 2013
Pressure at $r = 1,275$ km, $p_{1,275}$	2.16 ± 0.02 μbar	2.30 ± 0.01 μbar
Time of closest geocentric approach	04:13:37.24±0.07 UT	08:22:27.11±0.09 UT
Distance of closest geocentric approach[6]	-404.6 ± 2.7 km	-723.5 ± 2.7 km

Final Temperature Profile

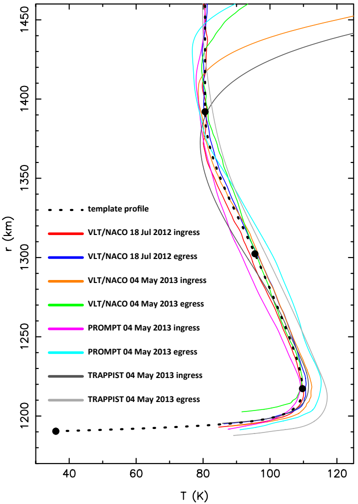

Fitted Light-curves

04:13 UT

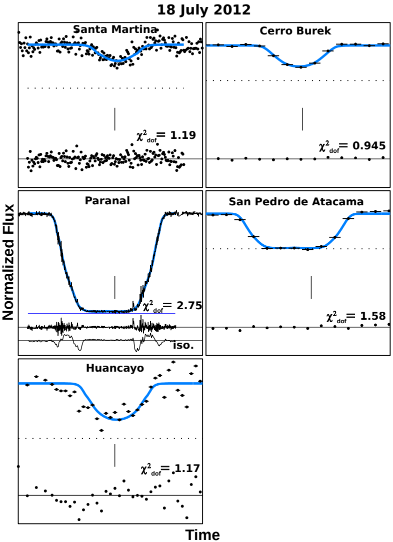

Fitted Light-curves

08:22 UT

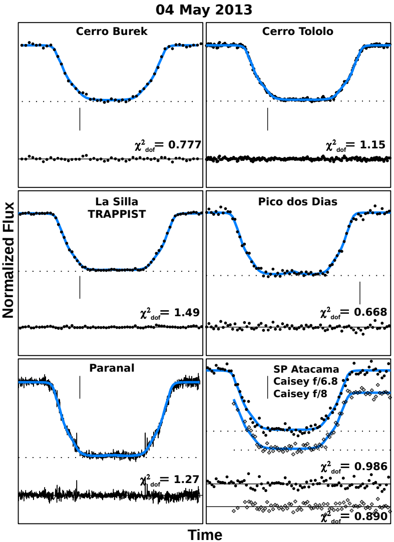

Radius determination

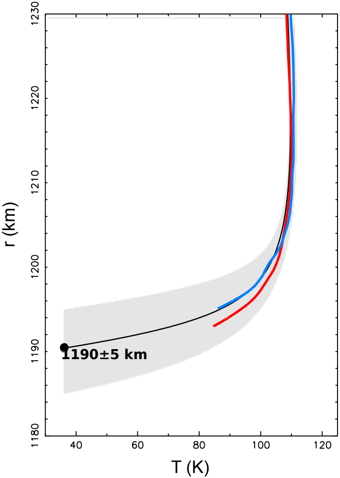

Possible cooling by CO or HCN

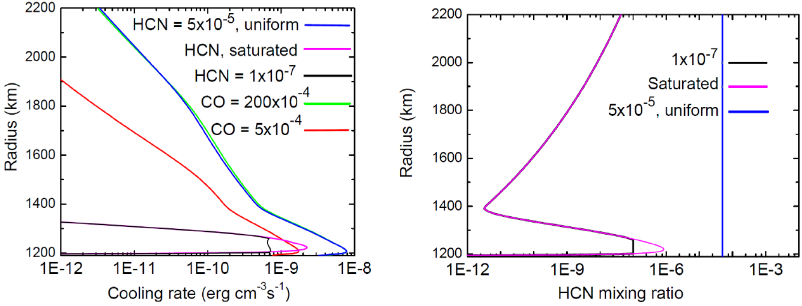

Conclusions

Conclusions

- Combination of well-sampled occultation chords and high SNR data, have allowed us to constrain the density, temperature and thermal gradient profiles of Pluto's atmosphere, between radii $r \sim 1{,}190$ km (pressure $p \sim 11\ \mu$bar) and $r \sim 1{,}450$ km (pressure $p \sim 0.1\ \mu$bar).

Conclusions

- Combination of well-sampled occultation chords and high SNR data, have allowed us to constrain the density, temperature and thermal gradient profiles of Pluto's atmosphere, between radii $r \sim 1{,}190$ km (pressure $p \sim 11$ μbar) and $r \sim 1{,}450$ km (pressure $p \sim 0.1$ μbar).
- We find that a unique thermal model, can fit satisfactorily twelve light-curves observed in 2012 and 2013, assuming a spherically symmetric and clear (no haze) atmoshere.

Conclusions

- The absolute vertical scale of our global model has an internal accuracy of about ± 1 km. However, this error is amplified to ± 5 km at the bottom of the profiles, because of the uncertainty on the residual stellar flux in the central part of the occultation observed by NACO on 18 July 2012.

Conclusions

- The absolute vertical scale of our global model has an internal accuracy of about ± 1 km. However, this error is amplified to ± 5 km at the bottom of the profiles, because of the uncertainty on the residual stellar flux in the central part of the occultation observed by NACO on 18 July 2012.
- In the frame of our model (i.e. assuming a constant temperature profile), we detect a significant 6% pressure increase (at the 6-σ level), during the $\sim$9.5 months separating the two events under study. This means that Pluto's atmosphere was still expanding at that time, confirming the work of Olkin et al. (2015), which compiles and analyzes pressure measurements between 1988 and 2013.

Conclusions

- The extrapolation of our temperature profiles to the nitrogen saturation line, implies that nitrogen may condense at a Pluto's radius of $R_P = 1{,}190 \pm 5$ km.

Conclusions

- The extrapolation of our temperature profiles to the nitrogen saturation line, implies that nitrogen may condense at a Pluto's radius of $R_P = 1{,}190 \pm 5$ km.
- From a Pluto's mass of $M_P = 1.304 \pm 0.006 \times\ 10^{22}$ kg (Tholen et al., 2008), we derive a density $\rho_P = (1.802 \pm 0.007)(R_P/1{,}200\ \mathrm{km})^{-3}$ g cm^{-3}. Our estimation thus implies $\rho_P = 1.85 \pm 0.02$ g cm^{-3}. This is larger, but not by much, than Charon's density, $\rho_C = 1.63 \pm 0.05$ g cm^{-3}.

Conclusions

- Above the stratopause, and up to about 1,390 km, our best 2012 and 2013 occultation light-curves yield inverted temperature profiles with a negative thermal gradient close to -0.2 K km^{-1}, which amounts to a total decrease of 30 K for the temperature between 1,215 and 1,390 km

Conclusions

- Above the stratopause, and up to about 1,390 km, our best 2012 and 2013 occultation light-curves yield inverted temperature profiles with a negative thermal gradient close to -0.2 K km^{-1}, which amounts to a total decrease of 30 K for the temperature between 1,215 and 1,390 km
- Explaining this negative gradient by CO cooling requires a mixing ratio (200×10^{-4}), that is too high by a factor of 40 compared to current measurements (Lellouch et al., 2011). Cooling by HCN is also discussed in this paper. It appears to be a possible alternative solution, but only if it remains largely supersaturated in the mesosphere.

Conclusions

- The *New Horizons* flyby data will provide constraints on the temperature boundary conditions and atmospheric composition that will be used to discriminate between the various solutions decribed here.

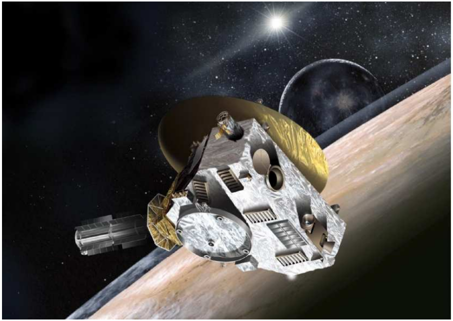

Assafin, M., Camargo, J.I.B., Vieira Martins, R., Andrei, A.H., Sicardy, B., Young, L., da Silva Neto, D.N., Braga-Ribas, F., 2010. Precise predictions of stellar occultations by Pluto, Charon, Nix, and Hydra for 2008-2015. Astron. Astrophys. **515**, A32.

Brosch, N., 1995. The 1985 stellar occultation by Pluto. Mon. Not. R. Astron. Soc. **276**, 571–578.

Elliot, J.L., Dunham, E.W., Bosh, A.S., Slivan, S.M., Young, L.A., Wasserman, L.H., Millis, R.L., 1989. Pluto's atmosphere. Icarus **77**, 148–170.

Hubbard, W.B., Hunten, D.M., Dieters, S.W., Hill, K.M., Watson, R.D., 1988. Occultation evidence for an atmosphere on Pluto. Nature **336**, 452–454.

Lellouch, E., Stansberry, J., Emery, J., Grundy, W., Cruikshank, D.P., 2011. Thermal properties of Pluto's and

Charon's surfaces from Spitzer observations. Icarus **214**, 701–716.

Olkin, C.B., Young, L.A., Borncamp, D., Pickles, A., Sicardy, B., Assafin, M., Bianco, F.B., Buie, M.W., de Oliveira, A.D., Gillon, M., French, R.G., Ramos Gomes, A., Jehin, E., Morales, N., Opitom, C., Ortiz, J.L., Maury, A., Norbury, M., Braga-Ribas, F., Smith, R., Wasserman, L.H., Young, E.F., Zacharias, M., Zacharias, N., 2015. Evidence that Pluto's atmosphere does not collapse from occultations including the 2013 May 04 event. Icarus **246**, 220–225.

Olkin, C.B., Young, L.A., French, R.G., Young, E.F., Buie, M.W., Howell, R.R., Regester, J., Ruhland, C.R., Natusch, T., Ramm, D.J., 2014. Plutos atmospheric structure from the July 2007 stellar occultation. Icarus **239**, 15–22.

Sicardy, B., Ortiz, J.L., Assafin, M., Jehin, E., Maury, A., Lellouch, E., Hutton, R.G., Braga-Ribas, F., Colas, F., Hestroffer, D., Lecacheux, J., Roques, F., Santos-Sanz, P., Widemann, T., Morales, N., Duffard, R., Thirouin, A., Castro-Tirado, A.J., Jelínek, M., Kubánek, P., Sota, A., Sánchez-Ramírez, R., Andrei, A.H., Camargo, J.I.B., da Silva Neto, D.N., Gomes, A.R., Martins, R.V., Gillon, M., Manfroid, J., Tozzi, G.P., Harlingten, C., Saravia, S., Behrend, R., Mottola, S., Melendo, E.G., Peris, V., Fabregat, J., Madiedo, J.M., Cuesta, L., Eibe, M.T., Ullán, A., Organero, F., Pastor, S., de Los Reyes, J.A., Pedraz, S., Castro, A., de La Cueva, I., Muler, G., Steele, I.A., Cebrián, M., Montañés-Rodríguez, P., Oscoz, A., Weaver, D., Jacques, C., Corradi, W.J.B., Santos, F.P., Reis, W., Milone, A., Emilio, M., Gutiérrez, L., Vázquez, R., Hernández-Toledo, H., 2011. A Pluto-like radius and a high albedo for the dwarf planet Eris from an occultation. Nature **478**, 493–496.

Tholen, D.J., Buie, M.W., Grundy, W.M., Elliott, G.T., 2008. Masses of Nix and Hydra. AJ, **135**, 777.

Vapillon, L., Combes, M., Lecacheux, J., 1973. The beta Scorpii occultation by Jupiter. II. The temperature and density profiles of the Jupiter upper atmosphere.. Astron. Astrophys. **29**, 135–149.